

M F F Nave et al

# Discharge Optimisation and the Control of Edge Stability

"This document is intended for publication in the open literature. It is made available on the understanding that it may not be further circulated and extracts may not be published prior to publication of the original, without the consent of the Publications Officer, JET Joint Undertaking, Abingdon, Oxon, OX14 3EA, UK".

"Enquiries about Copyright and reproduction should be addressed to the Publications Officer, JET Joint Undertaking, Abingdon, Oxon, OX14 3EA".

# Discharge Optimisation and the Control of Edge Stability

M F F Nave<sup>1</sup>, P Lomas, G T A Huysmans, B Schunke,  
B Alper, D Borba<sup>1</sup>, B de Esch, C Gowers, H Guo,  
T Jones, M Keilhacker, V V Parail, F Rimini,  
P Smeulders, P Thomas.

JET Joint Undertaking, Abingdon, Oxfordshire, OX14 3EA, UK.

<sup>1</sup>Associação EURATOM/IST, Lisbon, Portugal.



## ABSTRACT

Discharge optimisation for improving MHD stability of both core and edge was essential for the achievement of record fusion power discharges, in the ELM-free hot-ion H-mode regime, in the recent JET deuterium-tritium operation. In this paper the techniques used to increase edge stability are described. In particular the paper reports on the successful technique of current ramp-down used to suppress the outer mode. The increased stability of the outer mode by decreasing the edge current density confirms its identification as an  $n=1$  external kink [1]. Decreasing the plasma current, however, decreases the ELM-free period, which is consistent with stability calculations that show an earlier onset of the ballooning limit. In order to increase external kink stability without deteriorating the ELM-free period, a compromise was achieved by using plasma current ramp-down, while working at the highest plasma current values possible. Results from a plasma current scan show that at the time of occurrence of the first giant ELM, the plasma stored energy as well as the pressure measured at the top of the edge pedestal increase linearly with plasma current, for a given plasma configuration and power. This is consistent with models of the edge transport barrier, where the transport barrier width is proportional to the ion (or fast ion) poloidal Larmor radius. The MHD observations in deuterium-tritium and deuterium only discharges were found to be similar. Thus the experience gained on the control of MHD modes in deuterium plasmas could be fully exploited in the deuterium-tritium campaign.

## 1. INTRODUCTION

JET ELM-free hot-ion H-modes [2, 3] are limited by magneto-hydro-dynamic (MHD) instabilities in the plasma core, associated with the sawtooth instability, as well as by instabilities near the edge such as outer modes and edge localised modes (ELMs) [4]. In order to reach the stored energy, and hence fusion performance, expected from the underlying confinement, the MHD phenomena should be suppressed. Experimental results show that the best performance is obtained when both core and edge MHD phenomena occur late in the heating phase.

The Hot-ion H-mode regime describes plasmas where the ion temperature exceeds the electron temperature, by factors of 2-3, over a large portion of the plasma volume. This is obtained by heating low density plasmas with neutral beam injection (NBI). These plasmas are characterised by an ELM-free period, when the total plasma stored energy, as well as the edge pedestal pressure, rise until limited by an MHD event. Edge MHD phenomena, outer modes and giant ELMs, have been a main concern, since they account for over 70% of the performance limitations observed in this regime [4], whilst the remaining plasmas are limited by large sawtooth crashes.

In JET Hot-ion H-mode discharges, large pressure gradients and large associated bootstrap currents develop at the edge of the plasma. Ballooning and kink stability analysis of several discharges shows that, in general, both outer modes and ELMs occur near the external kink

marginal stability. The outer mode is observed first, then as the edge pressure approaches the ballooning limit the first giant ELM is observed. At relatively low shaping, with typical triangularity  $\delta \sim 0.35$  and, at low values of the poloidal beta parameter,  $\beta_{\text{pol}} \sim 1$ , there is no access to the second stability region, since external kink modes become unstable well before the edge becomes second stable to ballooning modes [5]. This is quite different from DIII-D [6, 7] and C-MOD [8, 9] results where confinement limitation due to giant ELMs is observed when the edge is in the second stability regime.

MHD modelling has indicated several possible paths to increase the edge stability and, although, it has not been possible to eliminate entirely the MHD modes, successful measures have been taken to delay their onset. In particular this paper will report on the application of controlled reduction of the plasma current (current ramp-down) to the stabilisation of the outer modes, and on the effect of the plasma current itself on raising the threshold for the occurrence of the ELM. The technique of current ramp-down, where the flat-top plasma current value is reduced with a rate  $dI_p/dt \sim 0.3-0.5$  MA/s, has been used routinely as a discharge optimisation technique during hot-ion H-mode operation with the JET MKII divertor [10]. Instead of the irreversible collapse of the hot-ion H-mode regime which used to be observed at the onset of outer modes [4], plasma current ramp-down, either delays the outer modes or decreases their amplitudes, with a substantial improvement in neutron yield. Once the outer mode has been delayed, the duration of the high performance phase is determined by the time when the first giant ELM appears. Unfortunately, as it will be shown, decreasing the plasma current has an adverse effect on the onset of the giant ELM. Plasma current scans show quite clearly that the ELM-free period increases when the plasma current is increased. A compromise was achieved by using current ramp-down, while working at the highest plasma current values possible. These techniques for careful control of edge (and core MHD activity, which is presented in a separate paper [11]) were exploited in the recent deuterium-tritium (D-T) campaign (the DTE1 campaign [12]), to demonstrate both high fusion yield [13] and significant alpha particle heating [14].

This paper is organised as follows. In section 2 of this paper, an overview of the MHD modes observed in the high performance phase of a hot-ion H mode is given. This is followed by a more detailed description of the modes observed at the edge at the termination of the high performance phase. (MHD observations in the JET optimised shear plasmas are the subject of a separate paper [15]). In section 3 results of different plasma configuration scans showing a clear effect on the onset of the edge MHD activity are summarised. In section 4 we will show a comparison of both observations and stability calculations for discharges with and without current ramp-down. The effect of decreasing the plasma current on both outer modes and ELMs is discussed. In section 5, the results of a plasma current scan are shown. In particular the dependence of the edge pressure and the ELM-free period on plasma current are discussed. The MHD activity observed in the high performance D-T pulses is described in section 6.

## 2. MHD OBSERVATIONS

### 2a. MHD overview

The rich variety of MHD modes observed in the JET ELM-free plasmas with frequencies up to 125kHz and their correlation with changes in the neutron rate, has been described in two previous publications [4,16]. More recently, the installation of magnetic pick-up coils which measure fluctuations up to 1 MHz, during a time window of 4 s, provided a more complete view of the evolution of the MHD activity throughout a hot-ion H-mode plasma. It has also allowed a clear identification of high frequency modes, such as the toroidal Alfvén-eigenmodes (TAE) [17] and the “washboard” modes [18].

Figure 1 gives an overview of the MHD modes observed during the high performance phase of a discharge heated with a combination of neutral beam injection (NBI) and radio-frequency (RF) waves. It shows the spectra as a function of time obtained from the fast Fourier transform (FFT) of a Mirnov coil signal. The instabilities observed are indicated in the figure. Except for TAE modes seen in this discharge at frequencies larger than 300 kHz, all other modes observed at lower frequencies are typical of the MHD activity found in a hot-ion H-mode plasma with either NBI or combined heating. The TAE modes are only observed in discharges with RF power above 4 MW [19], and in NBI heated discharges at 1 MA, 1 T [20], where they have not been associated with any discharge degradation. Throughout the ELM-free period one can see a range of modes with frequencies between 40-200 kHz, named the “washboard modes” due to their characteristic signature in the FFT plots. These recently identified global modes and their possible effect on the underlying confinement are discussed in a separate paper [18]. The MHD modes which in most discharges have been associated with fast degradation of confinement and neutron yield are those

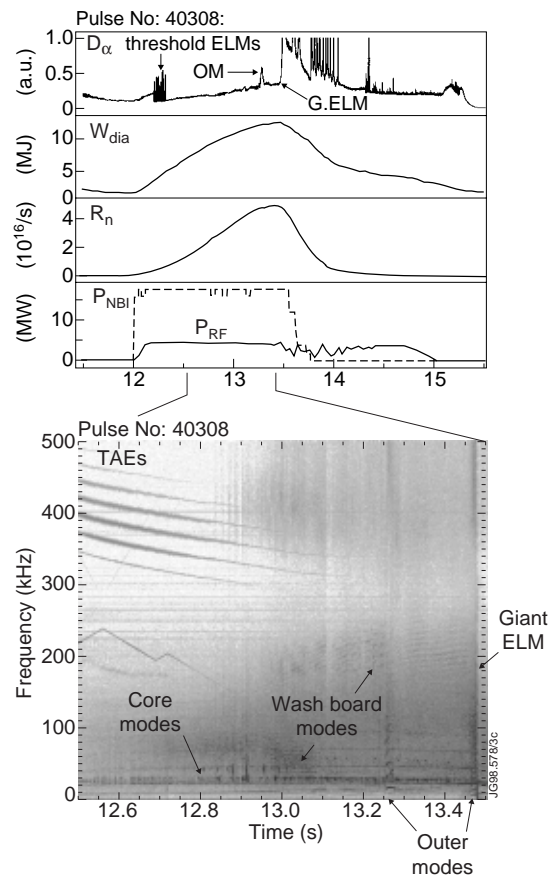


Fig.1: MHD activity observed in a deuterium hot-ion H-mode discharge developed as reference for the high performance DTE1 campaign. The boxes show (a) Temporal evolution of the neutron rate, plasma stored energy,  $D_\alpha$  emission and input auxiliary power. (b) Contour plot of a sequence of FFTs calculated from a magnetic signal. It shows the temporal evolution of the frequency of MHD modes during the high performance phase. The sea-saw like line around 200 kHz is the signal produced by the active Alfvén eigenmode excitation system using the saddle coil antenna [19].

observed at frequencies below 40 kHz such as sawtooth-related oscillations and outer modes, and the giant ELMs which are seen in the FFT plot as a fast broadband event. Figure 1 shows, throughout the heating phase, oscillations with frequencies of 20-30 kHz (corresponding to the frequency of rotation of the plasma core) related to fishbones and sawteeth. A sawtooth crash is not observed in this discharge, however large sawtooth crashes when present during the high performance phase, can cause irreversible saturation of the neutron rate [4,11]. At even lower frequencies, typically 5-10 kHz (the plasma rotation frequency at the edge), one finds edge modes referred to as “outer modes”. In figure 1, bursts of outer modes are observed at 13.24 s and 13.44 s. The second outer mode precedes the giant ELM which terminates the high performance phase in this discharge. Both outer modes and ELMs can be also identified by characteristic increases in  $D_{\alpha}$ , as seen in the top trace of figure 1.

N.B. Figure 1, shows an exceptionally good discharge, where the first outer mode burst does not prevent good performance. This has not always been the case as will be shown below.

## 2b. Observations of edge instabilities

“Outer mode” is the name given at JET to MHD oscillations observed around and beyond the  $q=3$  surface, with low toroidal mode numbers, the most typical being  $n=1$  with  $m=4-7$ . The mode structure observed in SXR data is described in detail in [1], where it is shown to be consistent with that of external kinks. Although the outer mode is localised near the edge, changes in plasma transport are observed in the core of the plasma, with a typical decrease in plasma stored energy of  $\sim 5\%$ . The largest effect, however, is observed in the central  $T_i$  and in the neutron yield. In some cases the hot-ion H-mode regime is totally lost (see examples given in ref. [4], where the hot-ion H-mode regime is terminated well before the onset of giant ELMs), in others the rise of the neutron yield is temporary clamped, as shown in figures 1 and 2. In most cases however, the confinement time and neutron yield fall short of their potential values. This is confirmed experimentally by comparing discharges limited by outer modes, with those where the mode is delayed, and also by predictive calculations with transport codes [4].

Figure 2 shows a discharge, where an outer mode starts at  $t=12.9$ s and lasts for 400ms. The outer mode is identified in the figure by an increase in the amplitude of the  $n=1$  magnetic signal and an increase in the  $D_a$  emission. The onset of the outer mode clearly clamps the neutron rate and the plasma stored energy, which were previously rising. It is also accompanied by an increase in the loss power ( $P_{\text{loss}} \cong P_{\text{NBI}} - dW_{\text{Dia}} / dt$ ). Although the mode is localised near the edge, a cold pulse propagating to the core of the plasma leads to an electron temperature collapse over a wide region. In figure 2,  $T_e$  decreases in the whole of the region outside  $q=1$ , with a clamping of  $T_e$  in the inner core. In the worst cases, a global  $T_e$  collapse is observed [4].

The final collapse of the neutron rate, with an irreversible loss of the ELM-free hot ion-H-mode regime occurs later (at  $t=13.75$  s) with a further onset of outer mode activity shortly followed by a giant ELM. This sequence of edge events in a JET ELM-free hot-ion H-mode is quite general, with outer modes being the first of the limiting MHD phenomena observed, then



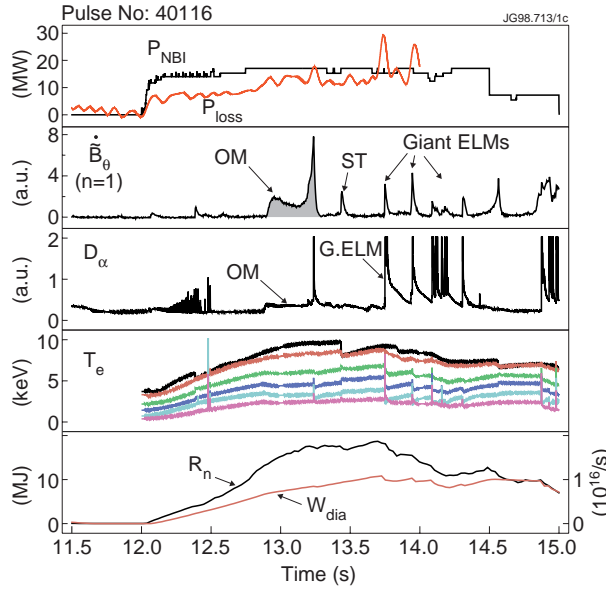


Fig.2: Temporal evolution of a deuterium ELM-free hot-ion H-mode discharge, with NBI heating, limited by an outer mode. From the top, the following traces are shown: input and lost power;  $n=1$  magnetic signal measured on the mid-plane low-field side showing perturbations associated with outer modes (OM), a sawtooth precursor (ST) and giant ELMs;  $D_\alpha$  signal showing bursts associated with edge MHD activity; electron temperature measured at different radii; neutron rate and the diamagnetic stored energy.

ELMy H-mode regime. (A description of type I ELMs [22] observed in JET steady state ELMy H-modes can be found in [23]).

It should be noted that outer modes and ELMs in the Hot-ion H-mode regime are closely related phenomena. A long lived outer mode (lasting 0.2-1.0 s), as the one shown in figure 2, will often trigger a small amplitude ELM (see  $D_\alpha$  trace in figure 2), possibly by temporarily increasing the edge pressure gradient. Unlike the giant-ELM which affect the whole plasma, this smaller ELM only affects the edge region. In a not yet understood way, it has the beneficial effect of suppressing the outer mode. At a later phase in the discharge when the outer mode is again observed, a giant ELM follows in a few milliseconds. Again it is probable that the outer mode has triggered the ELM, but that the ELM would have happened in any case, since even without the presence of an outer mode the pressure gradient at the edge appears to have reached a limiting value, as it will be discussed later in section 4b.

### 3. CONTROL OF THE EDGE MODES

Ballooning and kink stability analysis of several discharges shows that, in general, both outer modes and ELMs occur near the external kink marginal stability, with the first giant ELM observed as the discharge approaches the ballooning limit. Since both the ballooning and the external kink limits are important, stability analyses present several possible techniques to delay the

appearing again just before the giant ELM (as can be seen in figure 1). In some discharges the first onset of the outer modes is successfully suppressed, this will be shown later in section 4, where the discharge in figure 2 will be compared to a similar discharge optimised by current ramp-down.

The term giant ELM is here applied to edge MHD events associated with bursts of  $D_\alpha$  emission with amplitudes larger than  $10^{15}$  photons. $s^{-1}$ .sr $^{-1}$ .cm $^{-2}$ . A giant ELM is followed by a global temperature profile change, producing plasma stored energy losses up to 10% within  $\sim 100 \mu s$  [21], accompanied by a collapse of the neutron yield. If the hot-ion H mode has not been terminated by the initial outer mode, it is usually terminated at a later time by a second burst of outer mode activity followed by a giant ELM. Once the ELM-free period ends, the plasma usually enters a repetitive

edge MHD instabilities. The external kink may be controlled by parameters such as the edge plasma current density, the edge safety factor and the plasma inductance, while ballooning stability requires the control of the parameter  $\alpha$ , a normalised pressure gradient defined as  $\alpha = \mu_0 \nabla p / B_p^2$ , where  $p$  is the edge pressure and  $B_p$  is the poloidal field. Both the external kink and the ballooning stability can in principle be controlled by lowering the edge pressure gradient and by altering plasma shape parameters such as elongation, triangularity and edge shear.

Experiments in different plasmas configurations show that in all cases, i.e. independent of the type of the limiting MHD mode observed, the collapse of the hot-ion H-mode regime occurs at a similar critical value of the plasma inductance,  $l_i$ , with  $l_i^{\text{crit}} \approx 1$ . Since in these discharges  $l_i$  decreases during the heating phase, stability may be increased by slowing the reduction in  $l_i$  to this critical value. Care, however needs to be taken not to make the plasma core unstable to sawteeth. The input power is another important parameter, with both outer modes and giant ELMs occurring earlier as the power is increased. Typical times for the onset of edge MHD modes in 3.5T, 3.5MA discharges with input powers of 20MW, are  $\sim 1$  s into the heating phase for the outer modes, and  $\leq 1.5$ s for the first giant ELM. At a power of 10 MW, the ELM-free period increases to  $\leq 3.3$  s.

Experimentally, the most clear indication on how to increase the outer mode stability was found in experiments with current ramp-down (discussed in more detail in the next section), in toroidal field scans and using a cryo-pump.

Toroidal field scans at constant plasma currents have clearly shown that outer modes can be delayed and the neutron rate can be substantially improved by operating at higher  $q$  values.

Figure 3 shows the amplitude and time of onset of outer modes for different edge safety factors obtained from a  $B_t$  scan at a fixed plasma current of 1.6 MA. In this figure, the early and very large  $n=1$  mode for  $q_{95}=2.7$  locks and causes a disruption. As the toroidal field is increased, the onset of the outer mode is delayed and its amplitude is decreased. The amplitude of the magnetic field perturbations observed in the lower  $q$  examples in figure 3 are very extreme cases, and it explains why this domain is avoided for high performance hot-ion H-modes. Typical amplitudes of magnetic perturbations observed in the mid-plane at the low-field side, are those shown for  $q_{95} \sim 4.5$ , i.e.

$$\frac{\delta B_\theta}{B_\theta} \sim 10^{-4} \quad (\text{With a typical amplitude } \sim 10$$

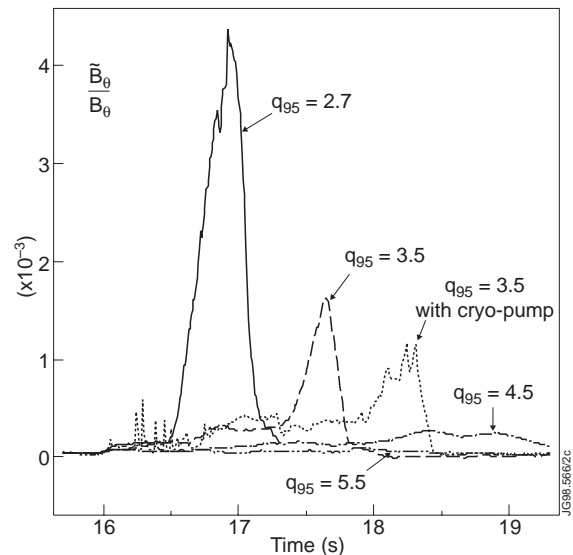


Fig.3:- Amplitude of outer-mode measured by a magnetic pick-up coil on the low-field side for a  $B_t$  scan at a fixed  $I_p=1.6$  MA,  $P_{\text{NBI}}=12.3$  MW. For  $q_{95}=3.5$  two similar discharges are shown with and without the use of the divertor cryo-pump.

times larger at the X-point [4]). The figure shows that in order to avoid outer modes it is better to have values of  $q_{95} \geq 5$ . A similar result was obtained in the more typical operation with  $I_p = 3\text{MA}$  reported in [4], where increasing  $B_t$  from 2.8T to 3.4T in a discharge with 19MW of NBI power, delayed the outer mode by 700ms allowing an increase in the neutron rate of 100%.

Scans at different plasma shapes, have not indicated significant differences in outer mode behaviour; they have however shown a clear impact on ELMs. The ELM free-period has been found to be lengthened by increasing triangularity and edge shear [24, 25]. Observations show that the ELM-free period increases with low recycling [26], indicating that the ELM may occur at a critical pressure gradient. A similar result has been obtained for outer modes, since comparison of discharges with and without the use of the cryo-pump show that low recycling can also make the outer mode more stable, as can be seen in figure 3.

A technique used routinely to improve performance during the MkII divertor operation was the continuous injection of gas at the edge of the plasma, referred to as gas bleeding, which increases the edge density and decreases the edge temperature. This has been found to reduce  $Z_{\text{eff}}$  in both ELM-free and ELMy-H-modes [27]. By cooling the plasma edge, and therefore decreasing the edge pressure, one could in principle increase both the stability of external kink and ballooning modes. However, the edge density increases faster than the edge temperature decreases, producing no net decrease in the edge pressure. Observations show that for the levels of gas used at present ( $10^{21}$ - $10^{22}$  electrons/s), gas bleeding does not affect the ELM-free period, while it has a small adverse effect of earlier onset of outer modes (this will be shown in section 4b).

## 4. THE CURRENT RAMP-DOWN TECHNIQUE

### 4a. Stabilisation of the outer modes

The external kink stability depends on the value of the current-density in the outer 5 cm of the plasma. Therefore, theoretical analysis suggests that a decrease in edge current-density, which could be achieved by decreasing the plasma current during the heating phase, improves the external kink stability and may delay the outer modes. This was indeed confirmed by experimental results. A comparison of discharges with and without current ramp-down clearly shows that in most cases, outer modes can be delayed, resulting in a substantial improvement in performance. This is illustrated in figures 4 and 5, where the discharge shown in figure 2 is compared with a similar discharge where the plasma current,  $I_p$ , was decreased during the heating phase, at a rate  $dI/dt = -0.4 \text{ MA/s}$ . With  $I_p$  ramp-down, the outer mode is delayed by 500 ms, in this particular case allowing an improvement in the neutron rate of 45%.

Transport and edge MHD stability analysis have been performed using the ideal MHD code MISHKA-1 [28], and transport codes TRANSP [29] (interpretation), JETTO [30] (predictive studies). Figure 5 shows the trajectory in the  $(\alpha, j_{\text{EDGE}})$  stability diagram for the two discharges compared in figure 4. The pressure gradient at the edge in JET is not measured, thus

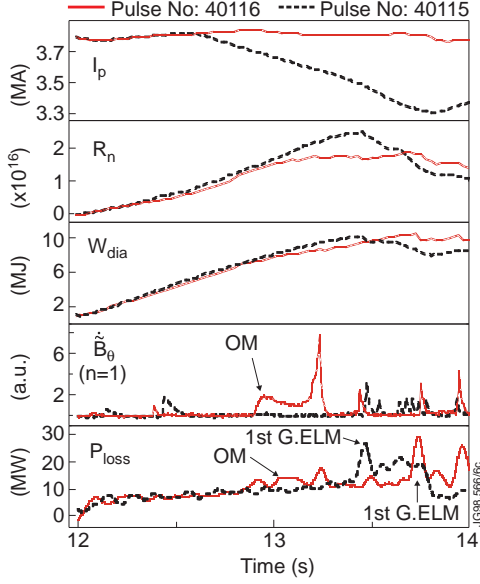


Fig.4: The discharge shown in figure 2 compared with a similar discharge where current ramp-down was used. With  $I_p$  decreased the outer mode is delayed by 500 ms, allowing an improvement in the neutron rate of 45%. However, the first giant ELM, which ends the high performance phase, occurs 300 ms earlier (see also figure 5).

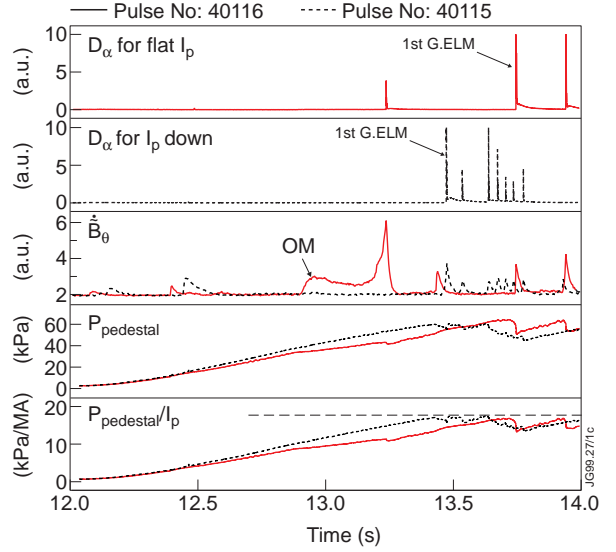


Fig.5: Comparison of edge measurements for the discharges with and without current ramp-down. The following traces are shown: (a)  $D_\alpha$  emission with the first giant ELM, i.e the first ELM that limits high performance, indicated; (b)  $n=1$  magnetic signal showing that outer mode is only observed in the case of  $I_p$  flat; (c) temporal evolution of the edge pressure at the top of the H-mode pedestal,  $P_{pedestal}=n_e(T_e+T_i)$ , measured at  $R=3.75$  m, i.e.  $\sim 5$  cm inside the separatrix; and (d) edge pressure at top of pedestal normalised to  $I_p$ .

both the edge pressure profile and the edge current density, including the contribution of a bootstrap term, are taken from numerical simulations which use the JET transport model described in [31]. The pressure profiles calculated numerically were compared with the experimental profiles, such that the calculated and measured pressures at the top of the edge pedestal (shown in figure 5) coincide within the experimental uncertainty of 20%. Figure 6 shows that with  $I_p$  ramped down, the plasma is more stable to external kinks. This is due to a change of sign in the electric field, which decreases the Ohmic current in the outer region, (figure 7). (The change in the bootstrap current is negligible.) Equilibrium calculations with EFIT [32] show increases around 10% in edge shear, edge safety factor and  $I_i$ , all contributing to increasing external kink stability.

Decreasing the plasma current as a way to increase  $\beta_N$  has also been used in machines such as TFTR [33] and ASDEX [34]. However, those experiments are quite distinct from the ones described here, since the plasma current is decreased by factors larger than 2, either before the auxiliary heating is on or very early in the heating phase. They report no change in the plasma stored energy while the plasma current is being decreased. In JET, the timing for the start of the current ramp-down was found to be very important. Since in a hot-ion H-mode the maximum achievable plasma stored energy scales with the plasma current (this will be shown in the

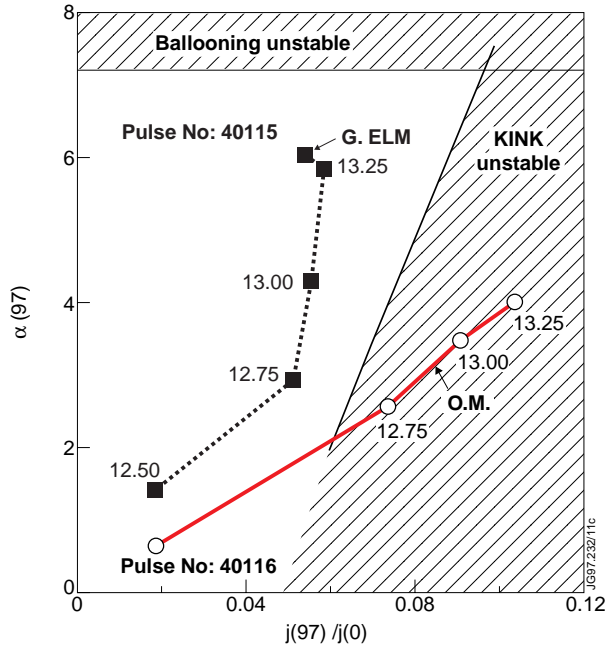


Fig.6: Trajectories in the  $(\alpha, j)$  diagram, for discharges shown in figure 4 and 5, with and without an  $I_p$  ramp. With  $I_p$  down the plasma is more stable to external kinks and more ballooning unstable. The current density is taken at 97% of the flux surface

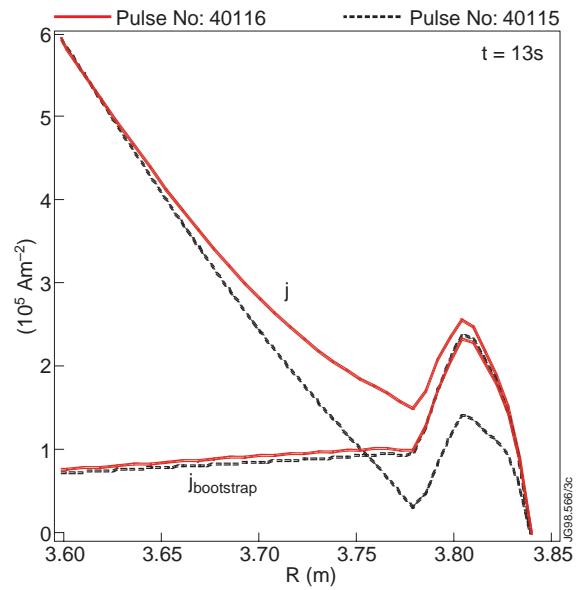


Fig.7: Comparison of the current density and current density bootstrap contribution in the outer region, simulated with the JETTO code.

next section), too large or too early a decrease in plasma current would have deteriorated the discharge. In JET, a small decrease in  $I_p$ , by typically 5%, starting 400-600 ms after the NBI power is switched on, is enough to suppress the outer mode. Figure 4 shows that a clear improvement in the plasma stored energy is obtained up to the time when the first ELM is observed.

#### 4b. The effect on the ELMs

For the large majority of discharges, the maximum values of the neutron rate and the plasma stored energy depend on the timing of the first giant ELM. Unfortunately, whilst the current ramp-down increases the time free of outer modes, observations show that the ELM-free period decreases. Figure 5 shows that in the discharge with the current ramp-down, the first giant ELM occurs 300 ms earlier. Although there is a substantial improvement in neutron rate, the maximum stored energy has actually been limited at a lower value than the one reached in the discharge with flat  $I_p$ .

The earlier occurrence of the giant ELM, is clearly illustrated in figure 8, where we show 3 pairs of discharges with and without current ramp-down. These discharges were designed to study the effect of gas bleeding on performance. Increasing the gas rate has a modest, unfortunately adverse, effect on the outer mode observed for constant  $I_p$ . Notice from comparing discharges 1a (large gas bleeding) with 3a (no gas bleeding), that the outer mode occurs 80 ms earlier. However gas bleeding has no effect on the ELM. Decreasing the plasma current, on the other hand,

has dramatic effects on both the occurrence of the outer mode and the ELM. Current ramp-down shows consistent results where the outer mode is stabilised while giant ELM activity occurs earlier. Comparing discharges 1a ( $I_p$  flat) and 1b ( $I_p$  ramp-down), one finds that the period free of outer modes was extended by 700 ms, while the ELM-free period was decreased by 200 ms.

The earlier appearance of the giant ELM in the experiments with current ramp-down, may be explained by an increase in the parameter  $\alpha \propto \nabla p / B_p^2$ , thus reaching the ballooning limit earlier, as shown in fig.6. There is typical decrease in poloidal field of  $\sim 10\%$ . In addition, by removing the outer mode the rate of rise of the pressure at the top of the pedestal does not saturate (fig.5). Thus, a critical edge pressure and, possibly a critical grad ( $p$ ) value as required by the ballooning limit, is reached earlier.

Figure 5 shows the evolution of the edge pressure measured at the top of the edge pedestal taken at a radius of 3.75 m (i.e. at  $\sim 5$ cm inside of the last flux surface). In the discharge with flat  $I_p$ , the outer mode temporarily clamps the edge pressure. Once the outer mode is quenched, the edge pressure continues to rise. In both discharges the maximum  $P_{\text{pedestal}}$  achieved is limited by the occurrence of the first giant ELM. The data indicates that at the time of the giant ELM, a critical  $P_{\text{pedestal}}/I_p$  value has been reached. To make this result consistent with the ballooning limit, would require that the width of the H-mode transport barrier would be proportional to  $I_p$ . This conclusion is also found from the analysis of discharges in a wider range of plasma current values, shown in the next section.

Since the giant ELM in this regime is preceded by an outer mode, and given the large experimental uncertainties in the calculation of the edge pressure gradients, it had not been possible up to now to say if the giant ELM was due to an external kink or to a ballooning limit. The observation of a giant ELM together with an outer mode indicates that at the time of the giant ELM, the trajectory in the  $(\alpha, j_{\text{EDGE}})$  diagram must have reached the top right-hand corner where both the external kink and ballooning marginal stability curves overlap. The different

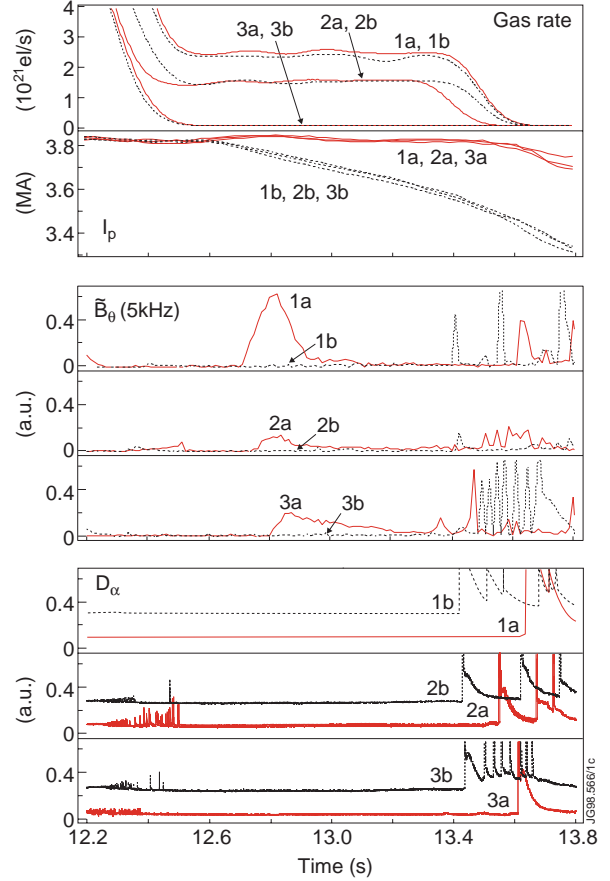


Fig.8: Pairs of discharges with and without current ramp-down for 3 different gas bleeding rates. The following plots are shown: (a) gas rates and total plasma current; (b) magnetic signals showing that with  $I_p$  reduced the outer mode is suppressed; (c)  $D_\alpha$  signals showing that with  $I_p$  reduced the first giant ELM occurs earlier. For the sake of clarity, an arbitrary constant has been added to the  $D_\alpha$  traces of the discharges with current ramp-down.

response that outer modes and ELMs have to the decrease of the edge current density in the current ramp-down experiments, as well as the results of stability analysis, indicate that for the giant ELM the ballooning limit, consistent with an appropriate transport barrier model, should be the most relevant.

## 5. THE ELM-LIMIT

The technique of ramping down the current was found to delay outer modes while making the giant ELMs appear earlier. Thus, from the point of view of controlling the giant ELMs, it is advisable to operate at the highest plasma current possible. This is also confirmed from experiments carried out at different values of plasma current, which show that the maximum plasma stored energy (fig.9), as well as the edge pressure (fig. 10) attained at the time of the first giant ELM are proportional to the plasma current. Fig. 10 shows that the pressure at the top of the edge pedestal, measured at 3.75 m, depends linearly on the plasma current, i.e.  $P_{\text{pedestal}} \approx \text{const } I_p^\alpha$ , where  $\alpha \approx 1$ . (The variation in edge shear is much smaller than in  $I_p$ , with all discharges in the range  $s_{95} \sim 3.3-4.1$ ). For the same plasma configuration, the maximum plasma stored energy increases with the level of input power, whilst the maximum value of  $P_{\text{pedestal}}$  is independent of power.

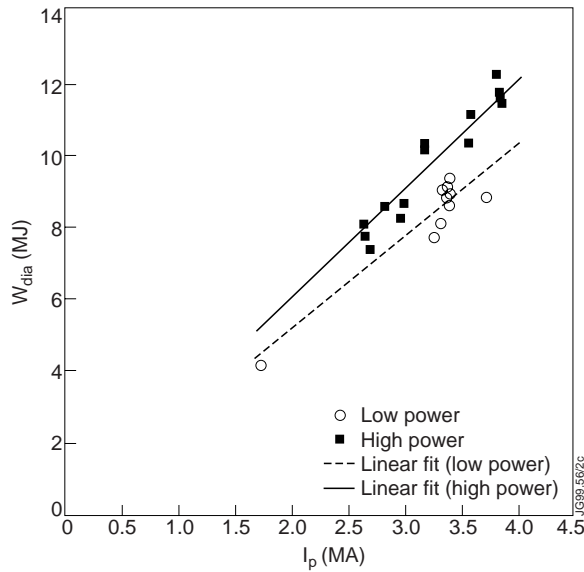


Fig.9: Plasma stored energy versus  $I_p$ , at the time of the 1st Giant ELM for deuterium discharges with NBI heating only, for two power levels: low power  $P_{\text{NBI}}=10$  MW, high power  $P_{\text{NBI}}=18-20$  MW

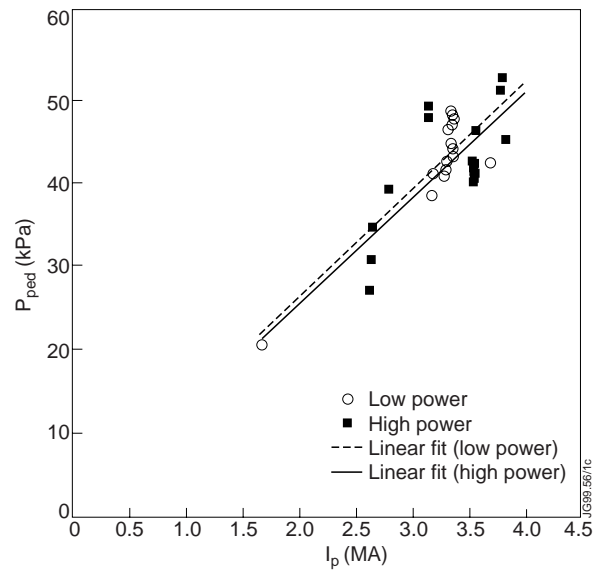


Fig.10: Pressure at the top of the edge pedestal, at  $R=3.75$  m, versus  $I_p$  at the time of the 1st Giant ELM, for the set of discharges shown in figure 9.  $P_{\text{pedestal}}$  in this graph includes dilution, i.e.  $P_{\text{pedestal}}=n_e T_e + n_d T_i$

The data also indicates that the time of occurrence of the first giant ELM is proportional to the plasma current (fig.11). At low power the ELM-free period increases, since it takes longer for the critical edge pressure to be reached. The scatter in this plot can be explained by how successfully the outer mode has been stabilised. In discharges with an untimely and large outer mode, the edge pressure can be clamped for several hundred milliseconds, as shown in figure 5.

This would increase the ELM-free period without improving performance. For instance, if one compares the two low power discharges shown in fig.11 at 3.2 MA, the one with the long  $t_{\text{ELM}} \sim 3.8$  s, has an early outer mode, which clamps the edge pressure for nearly one second. This delays the first giant-ELM actually leading to a lower stored plasma energy.

If for a given input power, the giant ELMs indeed occur at a limiting edge pressure gradient set by a ballooning limit, then the linear dependence of the edge pedestal pressure with the plasma current would indicate that the width of the transport barrier is also proportional to  $I_p$ . This behaviour suggests that the width of the transport barrier may scale as the ion (or fast ion) poloidal Larmor radius, as discussed in [35] for the JET ELM-free hot-ion H-modes and in [23, 36] for ELMy H-modes.

Notice that we have excluded from this discussion the smaller ELM which is some times seen following a long lived outer mode (as in the example with flat  $I_p$  in figures 4 and 5). Figure 5 shows that it can occur at a lower value than the critical  $P_{\text{pedestal}}$ . The hypothesis made is that the outer mode increases the edge pressure in a region further out where not all measurements needed to calculate the pressure are available. Some suggestion that this may be true comes from measurements in some discharges which show that  $T_i$  and/or  $T_e$  at the edge increase in the presence of the outer mode [37].

## 6. MHD OBSERVATIONS IN THE DEUTERIUM-TRITIUM DISCHARGES

Experiments in hot-ion H-modes during the recent JET D-T campaign (DTE1) were carried out at two different power levels: high power discharges, with 23-25 MW of combined RF and NBI heating designed to produce maximum fusion yield [13, 38] and, lower power discharges with 10 MW of NBI heating designed to study alpha particle heating [14]. The high performance discharges with a tritium concentration of 50% were produced in two configurations: 3.8 MA, 3.4 T and 4.2 MA, 3.6 T. The alpha-heating discharges with a wide range of tritium concentrations were in the standard 3.8 MA, 3.4 T configuration.

The MHD phenomena in the deuterium-tritium ELM-free discharges were found to be qualitatively the same as in deuterium only. This similarity was first observed in the 1991 PTE experiments in discharges with 10%T [16], and confirmed in DTE1 in discharges with tritium

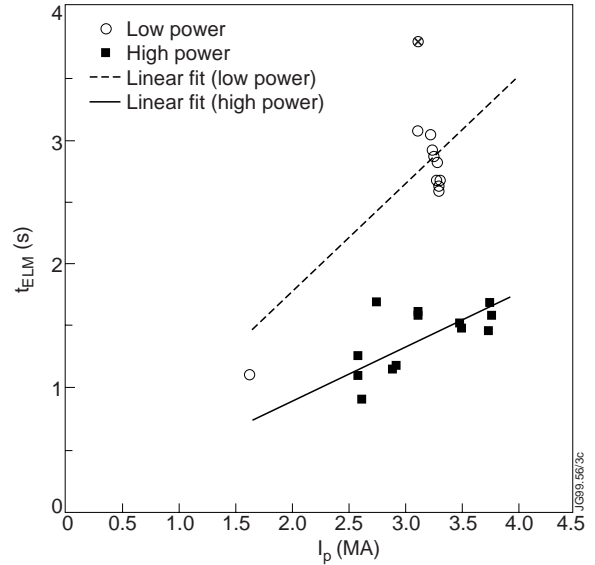


Fig.11: Time when first giant ELM is observed, with respect to the time when NBI is switched on, versus  $I_p$ . The low power discharge with  $t_{\text{ELM}}=3.8$ s (indicated by the symbol  $\otimes$ ) has a long lived outer mode, which clamps  $P_{\text{pedestal}}$  for nearly 1 sec, increasing  $t_{\text{ELM}}$ , without any gain in performance.



concentrations varying from 0 to 100% T. Careful control of edge MHD activity was therefore essential for the achievement of record fusion yields, and the previous acquired experience on how to increase stability has proved invaluable. Discharges were optimised by a careful choice of gas bleeding and a current ramp-down of  $-0.2$  MA/s (fig. 12).

Qualitatively, the most outstanding difference between MHD observations was in sawtooth behaviour. The sawtooth period was found to increase with tritium concentration [11]. With respect to edge MHD modes, in all DTE1 hot-ion H-mode discharges (i.e. both in high power and low power experiments), the termination of the high performance phase is caused by an outer mode combined with an ELM, similarly to their reference deuterium only discharges. Below, we will show results from the high power, high performance experiments with 50% T.

Figures 12 and 13 give a comparison of the highest performance D-T discharges, obtained in the two plasma current configurations, with deuterium-only reference discharges. Figure 12 shows discharge 42976 that produced the record fusion power of 16.1 MW and diamagnetic stored energy of 17 MJ in the higher plasma current configuration, while figure 13 shows the best discharge in the standard configuration, discharge 42676, which delivered a fusion power of 12.9 MW, and diamagnetic energy of 15 MJ. The figures show the following plots: total input power,  $D_\alpha$  signals showing increases in emission due to outer modes and ELMs, total plasma stored energy and edge pedestal pressure. Also shown in figure 12 are the loss powers and, in

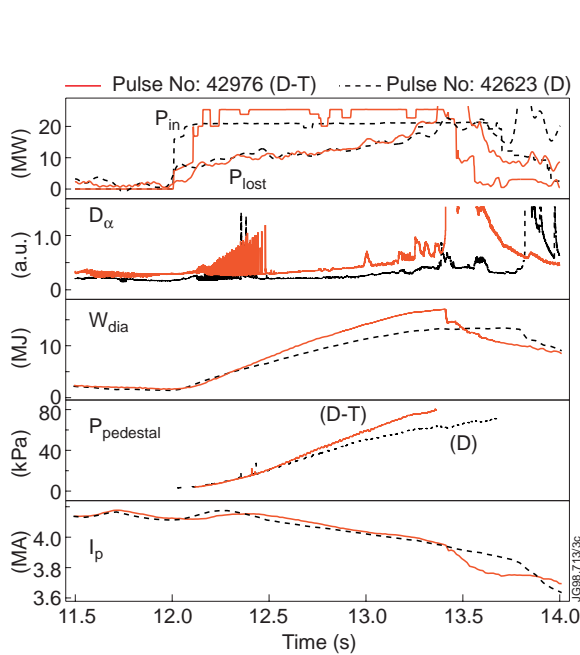


Fig.12: Record fusion power D-T discharge in the 4.2MA, 3.6T configuration, compared to a reference D discharge. Plots show: Total input power and lost power,  $D_\alpha$  emission, plasma stored energy, edge pressure at the top of the pedestal and, plasma current.

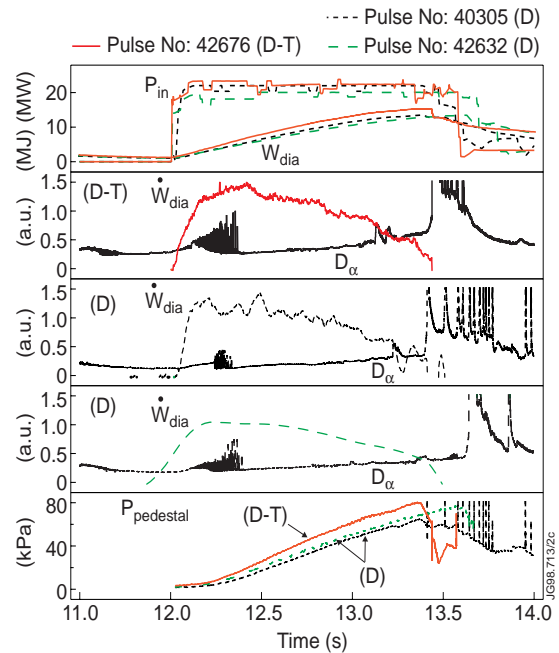


Fig.13: Record fusion discharge 42676 in the standard 3.8 MA, 3.4 T configuration compared to reference D discharges. The plots are as described in fig.11. Also included are plots of the derivative of the diamagnetic energy available for two of these discharges from a fast measurement. Two reference discharges are show to illustrate the variation in ELM-free period and edge pressures observed in deuterium.

figure 13 the derivative of the diamagnetic energy,  $\dot{W}_{\text{dia}}$ . As already seen in deuterium, in the presence of edge MHD modes, there is an increase in  $P_{\text{loss}}$ , due to a reduction in  $\dot{W}_{\text{dia}}$ . In both configurations it has been found that outer modes occur earlier in the D-T discharges, and typically the giant ELMs also appear earlier, however the differences observed between deuterium and D-T are within the variability found for similar deuterium discharges (as can be seen in figure 12.).

The differences in edge pressure as a function of tritium concentration in the low power alpha-heating experiments are discussed in [35]. It is shown that in the 10 MW NBI heated discharges, the maximum edge pressure attained in the 50-60 %T discharges is ~20% higher than in deuterium, i.e. twice the relative uncertainty of the measurement ( $\pm 10\%$ ). For the high power data, shown in figures 11 and 12, the pedestal pressure in D-T is only about 10% higher than the maximum pedestal pressure in the reference deuterium data for both 3.8 and 4.2 MA data which is comparable to the relative uncertainty of the measurement. Furthermore, there is a 15% variation in the maximum edge pressure in the deuterium data at 3.8MA. Thus, whilst this high power data is not inconsistent with the isotopic effect observed at low power and the interpretation in terms of a fast ion Larmor radius [35], neither does it provide any direct confirmation. In fact, the most noticeable isotopic effect clearly seen in both figures 11 and 12 is that the pedestal pressure rises more quickly in D-T than in deuterium-only and that therefore not surprisingly the ELM-free period is typically shorter in D-T.

## 7. CONCLUSIONS

MHD stability was essential in the design of the high performance D-T discharges which delivered record fusion powers during the JET DTE1 campaign. Since the ELM-free hot-ion H-mode plasmas are limited by several types of MHD phenomena, discharge optimisation has required a fine tuning of parameters, such that control of one mode would not be in detriment to the control of other types of instabilities or to overall confinement properties.

Experimental results have shown that it is possible to increase the edge stability of the ELM-free hot-ion H-mode plasmas, leading to considerable improvements in the neutron yield. In this paper we have reported on the techniques used to stabilise the outer mode (an  $n=1$  external kink), which has been a main concern for these discharges. The outer mode has been successfully delayed either by current-ramp down, or by operating at high  $q$  ( $q_{95} > 5$ ) and/or by the use of the divertor cryo-pump. Current ramp-down, in particular, was used as a standard optimisation technique for hot-ion H-modes throughout the MkII divertor operation, avoiding the earlier termination of the high performance phase, which used to be observed at the onset of outer modes, i. e. well before the end of the ELM-free period. In accord with theoretical predictions, observations showed that the controlled decrease of the plasma current delays the outer mode. When an outer mode is still observed, it occurs in short, low amplitude bursts, which cause no irreversible confinement degradation.

Overall these techniques have been able to delay the outer mode by up to 700 ms in high power discharges, allowing the neutron yield to continue to rise, and providing in some cases an improvement with respect to non-optimised discharges of up to 100%. Further improvements could be envisaged by modifications of the current density profile and by decreasing the edge pressure. It has been found that the collapse of the neutron yield in all discharges, occurs at a critical value of  $l_i \approx 1$ . Thus, one could improve performance by working at higher  $l_i$  values. Deuterium gas fuelling has not improved stability. However it should be worthwhile to explore the stabilisation effect on both the external kink and the ballooning modes, of further cooling of the edge, for instance by increasing edge radiation.

The technique of current ramp-down was found to delay outer modes while making the giant ELMs appear earlier. Thus, with this technique, the improvement in performance which can be achieved by delaying the outer mode is eventually halted by an earlier onset of a giant ELM. It is clear from observations at different values of the plasma current, that from the point of view of controlling the giant ELMs, it is better to operate at high plasma currents.

The different response of ELMs and outer modes to decreasing the edge current density suggests that these are two separate edge phenomena, solving a long standing question of whether the giant ELM in these regimes is caused by the external kink or the ballooning limit. In the current ramp-down experiments, the increased stability of outer modes is consistent with their identification as external kinks, while the earlier onset of ELMs indicates that the ELM occurs at the ballooning limit. Nevertheless, the giant ELM in these plasmas occurs in the presence of an outer mode, indicating that the ELM occurs at the top right-hand side of the  $(\alpha, j_{EDGE})$  diagram where the ballooning and external kink marginal stability curves overlap.

Plasma current scans show that the total plasma stored energy and the edge pedestal pressure, taken just before the first giant ELM vary linearly with the total plasma current. This plasma current dependence is consistent with models for the edge transport barrier where the width of the transport barrier is proportional to the ion Larmor radius. In discharges where the outer mode has been delayed, the ELM-free period is also found to increase linearly with the total plasma current. However, in discharges non-optimised, the clamping of the edge pressure caused by the outer mode increases the ELM-free period without any net gain in plasma stored energy and neutron yield. For a given plasma configuration, the critical edge pressure was found to be independent of input power. The ELM-free period on the other hand decreases with power as expected.

The edge MHD phenomena in the D-T discharges were found to be the same as in the deuterium only discharges. A comparison between D and D-T discharges with 50% T, with input powers of 23-25 MW, showed that no significant difference exists in the time of onset of either outer modes or ELMs. In addition these edge MHD phenomena occurred at similar values of the edge pressure (the edge pressure in D-T being  $\leq 10\%$  higher than in deuterium only). This similarity in MHD behaviour meant that the techniques for increasing edge stability developed in

deuterium could be fully exploited during the D-T campaign. Indeed it should be noted that the successful translation of performance from deuterium to deuterium-tritium provides ample testimony as to the maturity of understanding of the MHD phenomena, as documented in this paper.

## ACKNOWLEDGEMENTS

The authors acknowledge the contributions of all the JET staff to the successful DTE1 campaign.

## REFERENCES:

- [1] Huysmans et al., Nucl. Fusion **38** (1998) 179
- [2] Thomson, E. et al., Phys. Fluids B **5** (1993) 246
- [3] JET Team (presented by T. Jones), Plasma Phys. Control Fusion **37** (1995) A359
- [4] Nave et al., Nuclear Fusion **37** (1997) 809
- [5] G.Huysmans et al., in Controlled Fusion and Plasma Physics (Proc. 22nd Eur. Conf. Bournemouth, 1995), Vol. 19C, Part I, European Physical Society, Geneva (1995) 201
- [6] T.S.Taylor et al., 17<sup>th</sup> IAEA Fusion Energy Conference, Yokohama, Japan, 19-24 October 1998, IAEA-F1-CN-69/OV1/3
- [7] L.L.Lao et al., 17<sup>th</sup> IAEA Fusion Energy Conference, Yokohama, Japan, 19-24 October 1998, IAEA-F1-CN-69/EX8/1
- [8] A.E.Hubbard et al., Phys. Plasmas **5** (1998) 1744
- [9] R.S.Granetz et al., 17<sup>th</sup> IAEA Fusion Energy Conference, Yokohama, Japan, 19-24 October 1998, IAEA-F1-CN-69/EX6/2
- [10] The JET Team (presented by M. Keilhacker), Plasma Phys. Control Fusion **37** (1995) A3
- [11] Nave M FF et al., 25<sup>th</sup> EPS Conference on Controlled Fusion and Plasma Physics, Prague 29 June- 3 July (1998)
- [12] A.Gibson and the JET Team, Phys. Of Plasmas **5** (1998) 1839
- [13] Keilhacker et al, "High Fusion Performance from Deuterium-Tritium Plasmas in JET", submitted to Nuclear Fusion (1998)
- [14] Thomas P R et al., Physical Review Letters, **80**, 5548 (1998)
- [15] Huysmans, G. et al., "MHD stability of Optimised shear discharges in JET", submitted to Nuc. Fus. (1999)
- [16] Nave et al., Nuclear Fusion **35** (1995) 409
- [17] W. Kerner et al., Theory of Alfvén Eigenmode Instabilities and Related Alpha Particle Transport in JET Deuterium-Tritium Plasmas, Pre-print JET-P(98)04 (1998), to appear in Nuclear Fusion
- [18] P.Smeulders et al., "Characteristics of a new class of transport related MHD modes in JET H-mode plasmas", submitted to Plasma Physics (1999)
- [19] Fasoli, A. et al., Phys. Rev. Lett. **76** (1976) 1067

- [20] D. Borba et al, “Observation of Beam Driven Alfvén Eigenmodes in the Joint European Torus”, in preparation
- [21] Gill, R.D. et al, Nuclear Fusion, **38** (1998) 1461
- [22] Doyle, E.J. et al. Phys. Fluids B 3 (1991) 2300
- [23] V. Batnagar et al. “Edge localised modes and edge pedestal in NBI and ICRF heated H, D, and T plasmas in JET”, submitted to Nuc. Fus. 98
- [24] JET Team (presented by T. Jones), Plasma Physics and Control. Fusion **37** (1995) A359
- [25] T.C. Hender et al., in Controlled Fusion and Plasma Physics (Proc. 22nd Eur. Conf. Bournemouth, 1995), Vol. 19C, Part I, European Physical Society, Geneva (1995) 29
- [26] Lawson, K.D., et al., in Controlled Fusion and Plasma Physics (Proc. 22nd Eur. Conf. Bournemouth, 1995), Vol. 19C, Part II, European Physical Society, Geneva (1995) 77
- [27] G.Saibene, et al., in Controlled Fusion and Plasma Physics (Proc. 24th Eur. Conf. Berchtesgaden, 1997), Vol. 21A, Part I, European Physical Society, (1997) 49
- [28] A.B.Mikhailovskii et al., JET Report JET-P(96)25 (1996), accept for public. in Reports of Plasma Physics
- [29] R.J. Goldston et al., J.Comput. Phys. **43** (1981) 61
- [30] G. Cenacchi and A. Taroni, Raporto ENEA RT/T1B 88(5) 1988
- [31] The JET Team (presented by A. Taroni), 16<sup>th</sup> IAEA Conference, Montreal, Canada 7-11 October 1996, Fusion Energy vol.2 (1996) p.477
- [32] LAO, L.L. et al, Nuclear Fusion **30** (1990) 1035
- [33] S.A.Sabbagh et al., Phys. Fluids B 3 (1991) 2277
- [34] H.Murmann, H.Zohm, and the ASDEX- and NI Team, Proc. Of the 17<sup>th</sup> European Conference on Controlled Fusion and Plasma Heating, Amsterdam (EPS, Petit-Lancy, Switzerland, 1990), vol. 14 B, Part I, p. 54.
- [35] Guo et al , “Edge transport barrier in JET Hot-ion H-modes”, submitted to Nuc. Fusion (1998)
- [36] G. Saibene , “The influence of isotopic mass, edge magnetic shear and input power on high density ELMy H-modes in JET”, submitted to Nuc. Fus. (1998)
- [37] B.Alper et al., 25<sup>th</sup> EPS Conference on Controlled Fusion and Plasma Physics, Prague 29 June- 3 July (1998)
- [38] Rimini et al., Combined heating experiments in ELM-free H-modes in JET”, submitted to Nuc. Fusion (1999)